Disappearance of Roton Propagation in Superfluid ^{4}He at T_λ

E. C. Svensson
Atomic Energy of Canada Limited, Chalk River Laboratories, Chalk River, Ontario, Canada KOJ 1JO

W. Montfrooij
Netherlands Organization for Scientific Research (NWO), Den Haag, The Netherlands and ISIS Pulsed Source, Rutherford Appleton Laboratory, Didcot, OX11 0QX, United Kingdom

I. M. de Schepper
Interfaculty Reactor Institute, Delft University of Technology, Mekelweg 15, 2629JB Delft, The Netherlands
(Received 30 July 1996)

Using neutron scattering, we determine the dynamic structure factor $S(q, \nu)$ of liquid ^{4}He for the roton wave number $q = 2.0$ Å^{-1} as a function of frequency ν at constant density 0.1715 g cm^{-3} and for ten temperatures in the range $1.08 \leq T \leq 2.00$ K, primarily near the superfluid transition temperature $T_\lambda = 1.9202$ K. The superfluid transition is marked by a complete softening of the roton mode and a rapid decrease in lifetime. This change is continuous with temperature, and we find no evidence for a new mode appearing as one enters the superfluid phase, as has been proposed on the basis of theoretical considerations. [S0031-9007(96)01635-3]

PACS numbers: 67.40.–w, 05.30.–d, 67.20.+k

The temperature dependence of roton excitations in liquid ^{4}He near the superfluid transition temperature T_λ has been extensively studied by means of neutron scattering (for recent reviews, see [1]). Rotons are plane wave excitations in the fluid with wave number $q_r = 2.0$ Å^{-1} corresponding to the range of the interatomic potential $\sigma \simeq 2\pi/q_r = 3.1$ Å. A roton reveals itself as a peak in the experimentally observed dynamic structure factor $S(q, \nu)$ at $q = q_r$ and frequency $\nu = \nu_{\text{rot}}(T)$. For $T \lesssim 1$ K the roton peak in $S(q, \nu)$ at $\nu_{\text{rot}}(T)$ is extremely strong and sharp [1]. For increasing $T > 1$ K the width of the roton peak in $S(q, \nu)$ gradually increases while the frequency $\nu_{\text{rot}}(T)$ slowly decreases. At $T \geq T_\lambda$ (= 2.17 K at saturated vapor pressure) the width of $S(q, \nu)$ is much larger than the peak position. Thus one concludes that the roton peak in $S(q, \nu)$ is a signature of the superfluid phase of ^{4}He, although no sharp transition is observed directly in $S(q, \nu)$ on passing through T_λ [2].

Recently, Glyde and Griffin [3,4] postulated that the roton for $T < T_\lambda$ can be viewed as a renormalized single-particle mode typical of the superfluid state and physically different from the semiclassical density fluctuations observed in $S(q, \nu)$ for $T > T_\lambda$ [5]. Therefore one might expect distinct changes in $S(q, \nu)$ on passing through T_λ. Furthermore, these changes are expected to be such that they signal the appearance of a new excitation in the fluid when one enters the superfluid phase. The Glyde-Griffin model has been used extensively (see, e.g., [6,7]) to analyze recent neutron scattering results for liquid ^{4}He.

We present neutron scattering results for $S(q_r, \nu)$ for liquid ^{4}He at constant density $\rho = 0.1715$ g cm^{-3} (pressure $p \approx 20$ bar) for ten temperatures in the range $1.08 \leq T \leq 2.00$ K, with particular emphasis on temperatures very close to $T_\lambda = 1.9202$ K. A preliminary account of this work has been given previously [8]. These measurements were undertaken in order to study, much more thoroughly than previously, the evolution of the character of the roton excitation as one passes through the superfluid transition. The measurements were carried out using the N5-triple-axis spectrometer at the NRU reactor of the Chalk River Laboratories. The scattered neutron energy was fixed at $E/h = 1.19$ THz and Si(111) and pyrolytic graphite (002) planes were used for the monochromator and analyzer, respectively. The energy resolution at the energy transfers most relevant for our experiments was 0.06 THz (full width at half maximum). A sapphire filter at 77 K was placed in the incident beam to reduce the fast neutron background and a 6 in. beryllium filter at 77 K was placed in the scattered beam to prevent higher-order neutrons from reaching the detector. The effect of higher-order neutrons on the diffracted beam monitor was determined from a set of indium foil absorption measurements. We used a cylindrical aluminum pressure cell (4.45 cm inside diameter, with 0.05 cm wall thickness), which contained horizontal boron nitride absorbing disks spaced 1.6 cm apart to minimize multiple scattering. The results were corrected for multiple scattering and for scattering from the empty cell, allowing for the attenuation by the sample.

The temperature of the pressurized helium sample was established by controlling the vapor pressure of the helium bath to which the sample cell was thermally anchored. For all measurements, the helium bath was in the superfluid state, thereby giving excellent temperature uniformity of and heat conductivity through the bath. The temperature fluctuations in the sample cell were less than 0.0005 K in the superfluid phase, and less than 0.005 K in the normal phase. The superfluid-transition temperature

 0031-9007/96/77(21)/4398(4)$10.00

of the sample was measured (several times) by slowly lowering the temperature of the helium bath through the transition at T_λ of the sample and letting the cell warm up again, to detect the anomaly in the specific heat at T_λ. We find $T_\lambda = 1.9202 \pm 0.0002$ K on the scale of a calibrated germanium resistor immersed in the sample. In this way $T - T_\lambda$ of the sample was accurately determined and controlled. In this study we have probed to within 0.0026 K of T_λ from below, almost 10 times closer than in the only well-documented (as regards temperature accuracy) previous study [9]. Our approach from above, which is much less crucial, was to within 0.014 K.

The experimental results for $S(q_r, \nu)$ are shown in Fig. 1. For $T = 1.08$ K, one observes a sharp and strong roton peak at $\nu = 0.156$ THz, broadened by the experimental resolution. As T increases, the roton peak gradually broadens and the frequency, $\nu_{\rm rot}(T)$, slowly decreases. A broad peak at finite frequency is still observed above T_λ. There is no immediate indication of any major change in the character of the roton on passing through $T_\lambda = 1.9202$ K from the results for $S(q, \nu)$ shown in Fig. 1.

We analyze our data for $S(q, \nu)$ numerically using the memory function formalism (see, e.g., Chap. 9 of Ref. [4]). This formalism (which is formally equivalent to the projection formalism described in [5,10]) expresses the dynamic susceptibility $\chi(q, \nu)$ in terms of the memory kernel $M(q, \nu)$ as

$$\chi(q, \nu) = \frac{2\pi f_{un}^2(q)\chi(q)}{f_{un}^2(q) - \nu^2 - \nu M(q, \nu)}, \qquad (1)$$

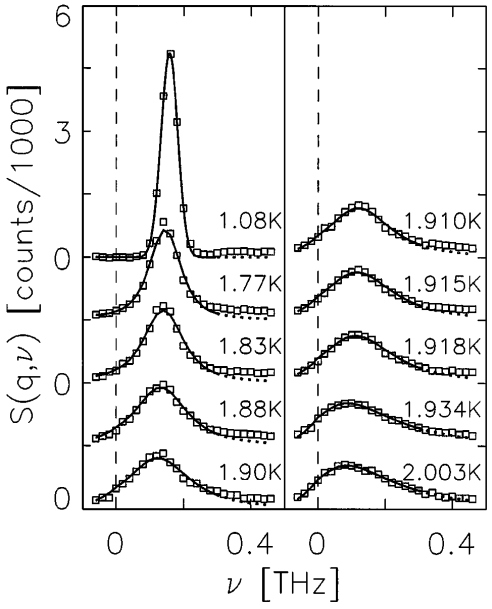

FIG. 1. $S(q, \nu)$ of liquid ^{4}He for $q_r = 2.0$ Å^{-1} at a constant density $\rho = 0.1715$ g cm^{-3}. The energy resolution is given by the width of the solid curve at 1.08 K. The results of the model fit (see text) for $\nu \leq 0.3$ THz are given by the solid curves, while the dotted curves are the extrapolation of the model to higher frequencies.

with $f_{un}^2(q) = M^{(1)}/M^{(-1)}$, and $M^{(n)}$ the nth frequency moment of $S(q, \nu)$. The static susceptibility is given by $\chi(q) = M^{(-1)}/(\pi h)$. In order to evaluate the temperature dependence of the poles of $\chi(q, \nu)$ which lie closest to the origin, we opt for a memory kernel $M(q, \nu)$ which is independent of frequency [i.e., $M(q, \nu) = i z_u(q)$]. We rewrite Eq. (1) in the form

$$\chi(q, \nu) = \frac{2\pi f_{un}^2(q)\chi(q)}{(\nu - \epsilon_+)(\nu - \epsilon_-)}, \qquad (2)$$

with $\epsilon_\pm$ given by

$$\epsilon_\pm(q_r, T) = \pm \sqrt{f_{un}^2(q_r, T) - z_u^2(q_r, T)/4} - i z_u(q_r, T)/2. \qquad (3)$$

In the case where $f_{un}(q) > z_u(q)/2$, this can be written as

$$\epsilon_\pm(q_r, T) = \pm \nu_s(q_r, T) - i\Gamma_s(q_r, T), \qquad (4)$$

where $\Gamma_s(q_r, T)$ is the roton damping and $\nu_s(q_r, T)$ is the roton propagation frequency. Note that $\nu_s(q_r, T)$ is only equivalent to $\nu_{\rm rot}(T)$ if $\Gamma_s(q_r, T) \ll \nu_s(q_r, T)$. However, if $f_{un}(q) < z_u(q)/2$, the propagation frequency becomes zero resulting in *two* diffusive (or overdamped) modes of different lifetimes [cf. Eq. (3)].

The memory kernel $z_u(q_r, T)$ of Eq. (2), which is none other than the damping rate of the momentum fluctuations, is obtained through a straightforward fitting procedure to the experimental data using Eq. (2) and the fluctuation-dissipation theorem [i.e., $\chi''(q, \nu) = (1 - e^{-\beta h\nu}) S(q, \nu)/2\hbar$]. Thus, we fit our neutron scattering data to the following model (which is convoluted with the measured experimental resolution function in the fitting procedure)

$$S(q, \nu) = \frac{2h\nu\chi(q)}{1 - e^{-\beta h\nu}} \frac{f_{un}^2 z_u}{(f_{un}^2 - \nu^2)^2 + (\nu z_u)^2}, \qquad (5)$$

with $\beta = (k_B T)^{-1}$, k_B being Boltzmann's constant. The above equation is identical to the one used in [5]; however, we have chosen the memory function description since this shows directly that the fitted parameters are poles of $\chi(q, \nu)$ [cf. Eq. (2)]. We apply the model to the region $\nu \leq 0.3$ THz so as to avoid the multiphonon region. Thus, we describe all our results for $S(q, \nu)$ using only a single variable parameter $z_u(q, T)$, since $\chi(q)$ and $f_{un}(q, T)$ are given by the sum rules for $S(q, \nu)$. However, because we disregard some of the intensity at higher energies (the multiphonon component), we find small deviations from the exact sum rules in the superfluid phase, reflecting the presence of the multiphonon component below T_λ. The results for $f_{un}(q_r, T)$ and $z_u(q_r, T)/2$ are plotted in Fig. 2, and the fitted values for $S(q, \nu)$ are shown by the solid curves in Fig. 1. It is clear from Fig. 1 that the model ($\nu \leq 0.3$ THz) gives a good fit for all temperatures and for both phases of the liquid. We have extrapolated the model to higher frequencies (dotted lines in

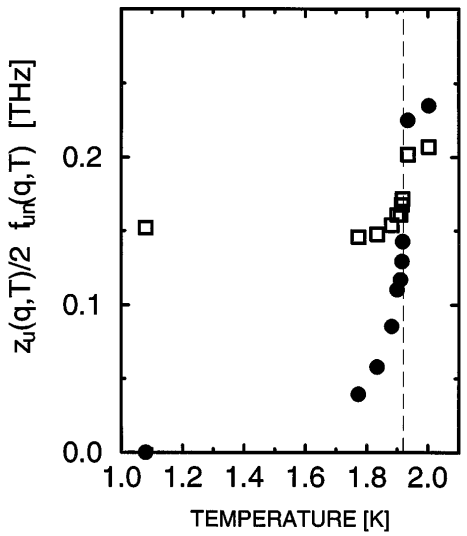

FIG. 2. $f_{un}(q,T)$ (squares) and $z_u(q,T)/2$ (circles) as a function of T. The superfluid transition temperature T_λ is indicated by the dashed vertical line. Note that $f_{un} = z_u/2$ at $T = T_\lambda$.

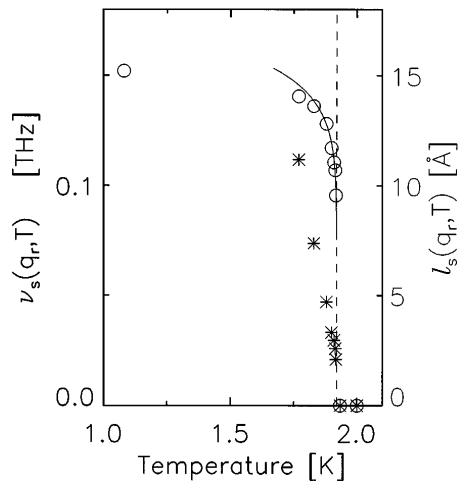

FIG. 3. The roton frequency $\nu_s(q_r,T)$ (circles) and the quantity $l_s(q_r,T)$ (asterisks) as a function of T. The change from propagating to nonpropagating behavior at T_λ (indicated by the dashed line) occurs in a very narrow temperature region. The solid curve is given by a power law fit which indicates that $\nu_s \propto (T_\lambda - T)^{0.1}$ as $T \to T_\lambda$. [A fit to $l_s(q_r,T)$ gives an "exponent" of $\approx 1/3$].

Fig. 1) to indicate the presence of the multiphonon contribution below T_λ. The results in Fig. 2 indicate that both f_{un} and z_u change *continuously* as a function of temperature. The increase with temperature of f_{un} reflects the disappearance of the multiphonon component, while the rapid change in the crucial parameter z_u reflects the dramatic change in damping rate of momentum fluctuations as one approaches and then crosses T_λ.

On increasing the temperature, we observe the following behavior of the parameters governing the roton mode: $f_{un} > z_u/2$ for $T < T_\lambda$ (propagating modes), $f_{un} = z_u/2$ for $T = T_\lambda$, and $f_{un} < z_u/2$ for $T > T_\lambda$ (overdamped modes). We illustrate this change from propagating to nonpropagating behavior in Fig. 3, where we plot the roton excitation energy as a function of temperature [cf. Eq. (3)]. For $T > T_\lambda$, the force f_{un} is too small compared to the rate of dissipation to sustain propagating modes in the fluid. Also plotted is the quantity $l_s(q_r,T)$ $\{= (2\pi/q_r)\nu_s(q_r,T)/\Gamma_s(q_r,T)\}$, which gives a measure of the spatial extent of the roton excitation, and which signals the transition from long range correlations to overdamped (diffusive) modes.

We conclude from our line shape analysis that the two roton modes of the fluid at $\pm\nu_s$ are propagating in the superfluid region ($T < T_\lambda$), merge at $T = T_\lambda$, and are nonpropagating for $T > T_\lambda$. This behavior is due to the sudden increase near T_λ of the damping rate $z_u(q_r,T)$ of momentum fluctuations (cf. Fig. 2). From the continuity of our description for $S(q_r,\nu)$ from $T > T_\lambda$ to $T < T_\lambda$ we conclude that in the roton region there is no indication of a new type of mode appearing as one enters the superfluid phase.

We emphasize that there is nothing in our analysis that could have forced the roton to go soft at T_λ. Our results, including the fitting to the values of $\nu_s(q_r,T)$ in Fig. 3 which gives a very small value (0.1) for the "critical exponent," show that there is a crucial change in the propagation character of the roton (driven by the change in damping rate) that occurs precisely at T_λ. This has not been observed previously. In fact, the changes in propagation frequency and character can be made visible to the naked eye by plotting the relaxation function $S_{\rm sym}(q,\nu)$, defined by

$$S_{\rm sym}(q,\nu) = \frac{1 - e^{-\beta h\nu}}{\beta h\nu} S(q,\nu)\,. \qquad (6)$$

The reason for this can be seen by rewriting Eq. (1) using the fluctuation-dissipation theorem. This leads to

$$S_{\rm sym}(q,\nu) = f(q)\,|\chi(q,\nu)|^2 {\rm Im}[M(q,\nu)]\,, \qquad (7)$$

with $f(q) = 8\pi^3 m/\beta h q^2$. Therefore, the poles of $\chi(q,\nu)$ are prominent features of $S_{\rm sym}(q,\nu)$. In special cases when $M(q,\nu)$ is only weakly frequency dependent in the region of interest, or when the low-lying poles of $\chi(q,\nu)$ are well separated in frequency from the higher energy ones, one can directly observe the behavior of the poles versus temperature. For liquid helium in the low temperature range, this is clearly the case due to the absence in the neutron scattering spectra of a mode corresponding to heat diffusion.

We determine $S_{\rm sym}(q,\nu)$ directly from our neutron scattering data [cf. Eq. (6)] and plot the results in Fig. 4 (not corrected for the experimental resolution function). The solid lines in this figure are merely guides for the eye. Independent of any line shape analysis, one can directly observe the *continuous* softening of the roton mode as T_λ is approached from below, combined with a rapid increase

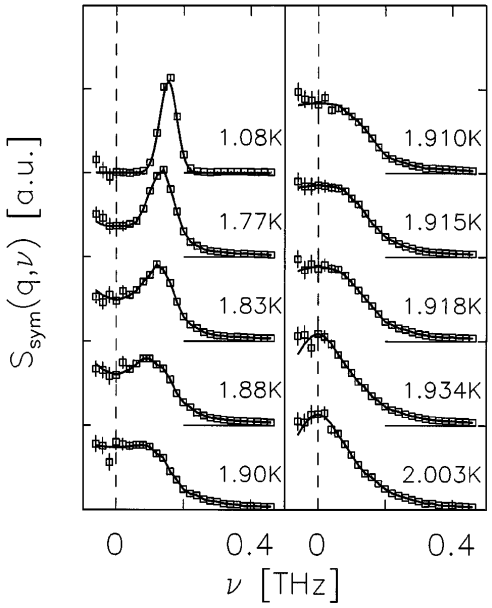

FIG. 4. The symmetric relaxation function $S_{\rm sym}(q,\nu)$ of liquid ^{4}He for $q_r = 2.0$ Å^{-1} (see text). The solid lines are guides for the eye.

in linewidth. The change takes place primarily in a small temperature region near T_λ, and appears to be completed at T_λ. We conclude with three remarks.

(1) For $T > T_\lambda$ the relaxation function $S_{\rm sym}(q,\nu)$ is centered around $\nu = 0$ and does not show any features of propagation (cf. Fig. 4). The fact that a peak at positive ν is seen in $S(q,\nu)$ for $T > T_\lambda$ (cf. Fig. 1) is simply a result of the asymmetric factor $f(\nu) = \beta h\nu/[1 - \exp(-\beta h\nu)]$ in the relation $S(q,\nu) = f(\nu)S_{\rm sym}(q,\nu)$ [cf. Eq. (6)]. Therefore, one should not attribute the peak seen in $S(q,\nu)$ for $T > T_\lambda$ to a propagating mode of the fluid.

(2) Dietrich *et al.* [2] found a sharp drop in $\nu_s(q_r,T)$ when approaching T_λ from below, similar to what we find here (cf. Figs. 3 and 4). However they did not find a vanishing of $\nu_s(q_r,T)$ for $T > T_\lambda$. This was mainly because of the different model fitting procedure they employed. We have strictly used Eq. (5) to describe our data, identifying the poles of $\chi(q,\nu)$ using Eq. (3) and thereby allowing for the possibility of two overdamped modes. What is most often encountered in the literature (see, e.g., [11]) is that the existence of a propagating mode is assumed *a priori*, and Eq. (4) is substituted into Eq. (5) for all temperatures, effectively ruling out the possibility of a nonpropagating roton mode above T_λ.

(3) Contrary to what had been inferred from earlier measurements [1] and is expected from theoretical considerations [3,4], we do not find any evidence for a renormalized single-particle mode replacing the regular density fluctuations of normal fluids as one goes below T_λ. This implies a qualitative disagreement with the interpretation proposed by Glyde and Griffin [3,4].

We thank D. C. Tennant, P. Moss, and M. Gauthier for expert technical assistance during the measurements.

[1] E. C. Svensson, in *Elementary Excitations in Quantum Fluids*, edited by K. Ohbayashi and M. Watabe (Springer-Verlag, Heidelberg, 1989); E. C. Svensson, in *Excitations in 2-Dimensional and 3-Dimensional Quantum Fluids*, A. F. G. Wyatt and H. J. Lauter (Plenum Press, New York, 1991).
[2] O. W. Dietrich, E. H. Graf, C. H. Huang, and L. Passell, Phys. Rev. A **5**, 1377 (1972).
[3] H. R. Glyde and A. Griffin, Phys. Rev. Lett. **65**, 1454 (1990).
[4] A. Griffin, *Excitations in a Bose-Condensed Liquid* (Cambridge University Press, New York, 1993).
[5] R. M. Crevecoeur, R. Verberg, I. M. de Schepper, L. A. de Graaf, and W. Montfrooij, Phys. Rev. Lett. **74**, 5052 (1995).
[6] K. H. Andersen and W. G. Stirling, J. Phys. Condens. Matter **6**, 5805 (1994).
[7] M. R. Gibbs and W. G. Stirling, J. Low Temp. Phys. **102**, 249 (1996).
[8] W. Montfrooij and E. C. Svensson, Physica (Amsterdam) **194B–196B**, 521 (1994).
[9] A. D. B. Woods and E. C. Svensson, Phys. Rev. Lett. **41**, 974 (1978).
[10] A. Griffin, Phys. Rev. Lett. **76**, 1759 (1996); R. M. Crevecoeur, I. M. de Schepper, and W. Montfrooij, Phys. Rev. Lett. **76**, 1760 (1996).
[11] E. F. Talbot, H. R. Glyde, W. G. Stirling, and E. C. Svensson, Phys. Rev. B **38**, 11 229 (1988).